



# Local atmospheric factors that enhance air-borne dispersion of coronavirus - High-fidelity numerical simulation of COVID19 case study in real-time

Kiran Bhaganagar<sup>\*</sup>, Sudheer Bhimoreddy

Department of Mechanical Engineering, University of Texas, San Antonio, TX, 78248, USA

## ARTICLE INFO

### Keywords:

Airborne  
Covid19  
Cough-jet  
Atmospheric dispersion  
Meteorology

## ABSTRACT

The spatial patterns of the spreading of the COVID19 indicate the possibility of airborne transmission of the coronavirus. As the cough-jet of an infected person is ejected as a plume of infected viral aerosols into the atmosphere, the conditions in the local atmospheric boundary layer together dictate the fate of the infected plume. For the first time - a high-fidelity numerical simulation study - using Weather-Research-Forecast model coupled with the Lagrangian Hybrid Single-Particle Lagrangian Integrated Trajectory model (WRF-HYSPLIT) model has been conducted to track the infected aerosol plume in real-time during March 9-April 6, 2020, in New York City, the epicenter of the coronavirus in the USA for comparing the morning, afternoon and evening release. Atmospheric stability regimes that result in low wind speeds, low level turbulence and cool moist ground conditions favor the transmission of the disease through turbulence energy-containing large-scale horizontal “rolls” and vertical thermal “updrafts” and “downdrafts”. Further, the wind direction is an important factor that dictates the direction of the transport. From the initial time of release, the virus can spread up to 30 min in the air, covering a 200-m radius at a time, moving 1–2 km from the original source.

## 1. Introduction

COVID-19 is an unprecedented global pandemic that originated in Wuhan, China in late December before spreading at a very rapid rate (WHO, 2019; WHO, 2020). In different geographical regions, the pandemic appears to be spreading at varying rates. COVID-19 clearly spreads more easily than other respiratory diseases (e.g., SARS Severe Acute Respiratory Syndrome). Micro-scaled virus particles that drift in the air or land on surfaces have multiplied into a global pandemic (Coronavirus disease, 2019). Air motions transport the micro-particles, with the extent of horizontal and vertical transport of the virus cloud depending on the wind conditions at that moment in time and at that location. The virus can reach the ground and potentially spread to someone passing through that region during the lifespan of the virus. On the other hand, if transported vertically away from the ground, it disperses and loses its affinity to affect healthy individuals.

### 1.1. Theoretical understanding on the role of meteorology on spreading of the COVID-19

Recent studies used statistical analysis to explore the correlation

between the local meteorological factors and the COVID-19 pandemic in various regions of the world. Transport of pollutant particles in the atmosphere due to turbulence dispersion is significantly higher than molecular dispersion resulting from fluid viscosity; in addition, the local meteorology dictates the trajectory and extent of a pollutant’s mixing in the atmosphere (Stull, 1993; Moeng and Sullivan, 1994). The studies considered air temperature, humidity, pollution levels, seasonal temperature as the main factors for the spread of the disease in their analysis. The accelerated spread of the disease in Northern Italy compared to the other regions till April 2020 can be attributed to meteorological conditions such as lower average wind speeds and low ambient temperatures (Coccia, 2020b, 2020c). The number of infections was higher in polluted cities than in cleaner cities (Coccia, 2020a).

However, due to the complex interaction of local meteorology, pollution and the viral infectivity which together influence the accelerated spread of the infection; hence to isolate pollution as the dominant factor is not appropriate. Further, Bontempi (2020) demonstrates that it is not possible to conclude that COVID-19 diffusion mechanism also occurs through the air, by using PM<sub>10</sub> as a carrier. The relation between seasonal temperature at the location and COVID-19 transmission was estimated using the ERA5 reanalysis product from European Center for

<sup>\*</sup> Corresponding author.

E-mail address: [kiran.bhaganagar@utsa.edu](mailto:kiran.bhaganagar@utsa.edu) (K. Bhaganagar).

Medium-Range Weather Forecasts (ECMWF), which provides daily gridded weather variables at the  $0.25^\circ$  latitude by  $0.25^\circ$  longitude resolution of 134 countries between [Jayaweera et al. \(2020\)](#) ([Carleton et al., 2020](#)). The study concluded that a  $1^\circ\text{C}$  increase in local temperature was associated with 13% fewer cases. COVID-19 growth rates were higher both in warmer/drier and colder/moist regions suggesting that both specific humidity and air temperature together influence the spreading of the virus ([Ficetola and Rubolini, 2020](#)). A cold and dry environment with low wind speeds is a more favorable condition for virus spreading ([Islam et al., 2020](#)). The spatial configuration of atmospheric circulation and stable atmospheric stability with dry conditions accelerated the viral spread by short-range droplet transmission ([Sanchez et al., 2020](#)). The lower mean air temperatures, dry conditions and calm winds are related to a higher number of cases and deaths in Southern Europe. Other studies have indicated the relation of low values of wind speed, humidity, and solar radiation exposure to a high rate of infection that support the virus's survival ([Ahmadi et al., 2020](#); [Eslami and Jalili, 2020](#)). In tropical regions there exists a higher correlation to wind speed and solar radiation to a higher incidence of the disease ([Rosario et al., 2020](#)). [Sarmadi et al. \(2020\)](#) correlated COVID-19 incidences to the higher latitudes and colder climates. Overall, though it is clear that in different regions of the world the meteorological factors including low wind speed, dry or moist climate with either hot or cold air temperatures and pollution in densely populated cities influenced the accelerated spatial spread of the virus, however, the relation between the various factors in regions of rapid transmission of COVID-19 pandemic has not been sufficiently investigated. In light of the existing studies, it is clear that certain atmospheric conditions favor the spread of the infection.

Turbulence is generated in the planetary boundary layer (PBL), the layer formed over the surface of the earth, due to the interactions of the surface heat and moisture flux. This turbulence influences the dispersion and transport of buoyant particle clouds released near the ground. Turbulence in the Planetary Boundary layer (PBL) is organized into accelerating air parcels (updrafts) and slower moving air parcels (downdrafts) that extend throughout the depths of the PBL when the PBL is in a convective regime ([Brown, 1980](#)). The particles released by an individual are carried by these updrafts and downdrafts, and the extent and direction of dispersion depends on the PBL dynamics. Further, under the influence of the wind shear of the three-dimensional wind vector, the buoyant cloud of particles expands in size as it entrains the surrounding area pockets and eventually becomes diluted. The distance traveled by the pollutant from the initial release point and the area covered from release to dilution depends on local PBL dynamics, such as turbulent advection processes, turbulent kinetic energy, and wind shear ([Stull, 1993](#)). Large-scale energy-containing turbulent eddies – coherent structures – are generally the size of the PBL's depth; they advect the pollutant through turbulent advection processes, and the smaller eddies mix them with the local atmosphere.

The virus needs moisture to survive, so the moisture content on the ground plays an additional role in allowing the virus to be active. Further, based on a recent study ([Van et al., 2020](#)) COVID-19 can live up to 4 days depending on the surface; the life span on cardboard is 24 h, on plastic 2–3 days, and on glass 4 days. It is very likely that the virus has a similar timeframe for survival on the ground. Overall, the transport of the infected micro-particles by atmospheric turbulence, the air-borne transmission of the disease, may represent an important pathway for pandemic spread. Little is known about the distance an infected patient's cloud can travel.

### 1.2. Virus particles released into the atmosphere

The cough/sneeze expectorant of a coronavirus-infected person releases respiratory droplets that contain infectious particles ([Centers for Disease Control and Prevention, 2020](#)). Research over the past decade has indicated that a person infected with respiratory disease, such as

influenza, releases a cough-jet with a significantly higher number of particles. Previous works have demonstrated that the average number of particles expelled by each cough for an infected patient can range from 900 to 302,200 ([Lindsley et al., 2012](#)). Furthermore, cough particles have a wide range of sizes, with different transport characteristics. Ongoing research on coronavirus has suggested that the cough-jet of a corona-infected patient could consist of aerosols, small particles suspended in air; these particles can survive in the air for several hours ([Van et al., 2020](#)). Another related study demonstrated that expectorants produce turbulent clouds of gas containing clusters of droplets that propel respiratory particles forward ([Bourouiba et al., 2014](#)). In fact, under optimal conditions, the droplets can travel up to 7–8 m indoors, which raises an important unanswered research question: How far can the blob of infected particles travel and how fast can it spread in outdoor spaces?

The goal of this study is to investigate the theory that buoyant blobs with coronavirus-filled particles (referred to as blob for the rest of the manuscript) released by infected patients' coughs are transported by turbulence processes before mixing and diluting into the atmosphere. The research question addressed is to quantify the scales of mixing (or diluting) of the virus-blob in terms of the atmospheric characteristics, i. e. atmospheric stability, wind conditions (wind shear, wind speed and wind direction), air turbulence, air/ground temperature and moisture content in the air. The length- and time scales of horizontal transport are analyzed using high-resolution simulations to understand the meteorological factors influencing the transport and mixing processes.

The objectives of the study are as follows:

1. To obtain detailed and accurate meteorological fields during the time of the release of the virus. For this purpose, Weather Research Forecast model simulations are conducted from March 9th to April 6th, 2020, in the New York City region to obtain wind conditions, atmospheric stability during that time.
2. To simulate transport of the virus particles in real-time: A Lagrangian model assists in simulating the transport of clusters of spherical, buoyant particles of size  $0.125\ \mu\text{m}$  with a half-life period of five days to quantify the transport of the infected blob subject to realistic atmospheric conditions at that location in real-time.
3. To characterize the dilution and dispersion of the particles in terms of the atmospheric state.

The posed research question will provide insights into a possible pathway for community transmission of the disease. Existing research clearly indicates the local air conditions, such as air circulation patterns, air temperature, and humidity, dictate the aerosol/blob of particles transported in the atmosphere. Turbulence is the most efficient mixing agent; the infected blob released into surrounding turbulent air currents is transported by turbulence, entraining ambient air, and becoming diluted. Atmospheric turbulence could transport the infection much faster and farther than would be possible in indoor conditions. As such, the present study seeks to use a high-resolution numerical model to obtain accurate air patterns in the New York region during the peak time period of COVID-19 in order to understand the transport processes influencing disease spread.

## 2. Methods and materials

### 2.1. Data and sources

We used high-resolution Advanced Research Version of the Weather Research Forecast Model (WRF-ARW v4.1) with realistic boundary conditions to simulate detailed atmospheric conditions in the region. The model was configured with three nested domains, as shown in Appendix Fig. 1. The model WRF to simulate PBL at scales similar to this study was previously tested and verified ([Bhimoreddy and Bhaganagar, 2018a, 2016b](#)). Domains D01, D02, and D03 were nested with the

feedback turned 'on' with horizontal resolutions 36 km (D01), 12 km (D02), and 3 km (D03). The model top was considered at 50 hPa with a total of 45 levels and 12 levels inside the PBL. The first grid point is at 24.08 m above ground. In the horizontal, D01 is discretized into a  $120 \times 120$  grid, D02 into  $105 \times 105$ , and D03 into  $103 \times 103$  grid points. The mesoscale runs were initialized at midnight 00 UTC on March 9, March 20, and April 1 of 2020, and run for a period of 7 days. Meteorological initial and boundary conditions for D01 were obtained from datasets provided by the National Centers for Environmental Predictions (NCEP) Global Forecast System Analyses (GFS-ANL), which has a horizontal resolution of 28 km; these measures were updated every 3-hrs. The GFS-ANL dataset was successful in initializing the WRF model when studying the dispersion of hazardous gas in Syria in 2017 (Bhaganagar and Bhimireddy, 2017). The model output for D03 was written every 30-min.

The dispersion model used was the Lagrangian Hybrid Single-Particle Lagrangian Integrated Trajectory model (HYSPPLIT model), which was set up with the grid center at 40.7114 N,  $-74.0017$  W, with a concentration grid spacing of  $0.0001^\circ$  ( $\sim 10$  m) in latitude and longitudinal directions with one vertical layer from 0 to 10 m above ground level. The overall concentration grid spans  $0.2^\circ$  ( $\sim 22$  km) in latitude and longitude. The meteorological input required to run the HYSPPLIT model was supplied by the WRF output from D03. To study the transport and dispersion, Lagrangian particles were released from 2 m elevation at the grid center. The particle emissions rate was set to  $1E7$  per hour and released for 0.01 h ( $\sim 36$  s). The particle concentration output from HYSPPLIT was measured in mass units per unit volume ( $\text{mass m}^{-3}$ ) and was collected every minute for a duration of 30 min from the time of release. Released particles are defined to be spherical in shape, with a diameter of  $0.125 \mu\text{m}$  and a density of  $1.7 \text{ g cm}^{-3}$ . The half-life of released particles is set to 5 days. Table 1 provides the details of the cases simulated in HYSPPLIT along with boundary layer height (PBLH), Monin-Obukhov length (MOL), and wind speed at 10 m at the time of release.

## 2.2. Morning, afternoon and evening release case studies

Three sets of WRF simulations were conducted in the New York City region (see Appendix Fig. 1) for the domain during the time periods of March 9–16, March 22–26, and April 1–6 to obtain a detailed micro-climatology of the region. The virus-blob was released at different time-instants in the PBL, and the trajectory of the particles was calculated in real-time for each instance of the release using a Lagrangian model. The virus-blob has been released at fifteen instances during this period which correspond to 1400 h on 03/11, 03/22, 03/12, 04/05, 04/02 (5 cases), 0700 h on 04/05, 04/02, 03/22, 03/12, 03/11 (5 cases) and 03/21, 03/11, 04/04, 04/01, 03/10 (5 cases).

**Table 1**

WRF simulations to obtain PBL characteristics at different release times of the virus between March 11, 2020–April 5, 2020. The columns correspond to  $\zeta$ , release date and time,  $T$ ,  $z$ ,  $L$ , wind-speed at 10 m height, wind shear close to the ground ( $dU/dz$ ), temperature gradient close to the ground ( $dT/dz$ ), TKE, and moisture content on the ground (amount of moisture per kg. of air).

$\zeta = Z/L$	Release (CDT)	$T$ ( $^\circ\text{K}$ )	$z$ (m)	$L$ (m)	$U10$ (m/s)	$dU/dz$ (1/s)	TKE ( $\text{m}^2/\text{s}^2$ )	$dT/dz$ ( $^\circ\text{K}/\text{m}$ )	$Q$ (kg/kg)
-30.78	03/11-1400	290.7	985	-32	3.1	0.02	0.66	0.05	3.5e-3
-22.16	03/22-1400	286.2	1330	-60	5.2	0.03	1.08	0.06	2.1e-3
-8.69	03/12-1400	289.8	800	-92	6.2	0.03	0.13	0.05	5.5e-3
-8.31	04/05-1400	292.7	665	-80	6.3	0.03	1.12	0.06	5.5e-3
-5.95	04/02-1400	290.6	1565	-263	10.2	0.03	2.63	0.05	3.5e-3
-5.28	04/05-0700	281.4	211	-40	1.9	0.01	0.15	0.01	5.5e-3
-3.5	04/02-0700	278.6	1022	-292	5.7	0.02	0.79	0.02	3.5e-3
-2.9	03/22-0700	274.6	749	-258	6.4	0.02	0.93	0.02	3e-3
-2.05	03/21-1900	280.1	1114	-542	5.3	0.01	0.61	0.006	2e-3
-1.44	03/12-0700	277.5	307	-213	2.6	0.008	0.18	0.005	4.5e-3
-1.4	03/11-0700	277.7	419	-300	4.2	0.01	0.39	0.01	3e-3
-1.39	03/11-1900	280.7	368	-265	4.4	0.01	0.45	0.008	7.5e-3
-1.25	04/04-1900	283.8	274	-220	3.5	0.0007	0.28	-0.0001	5.5e-3
0.63	04/01-1900	283.3	739	1182	5.2	0.002	0.62	-0.01	3.2e-3
2.75	03/10-1900	285.7	921	335	5.3	0.01	0.67	-0.03	7e-3

## 2.3. Data analysis procedure

### Estimating the dilution of the virus blob

The concentration output from the HYSPLIT model was given on the concentration grid. A value of  $1E-3$  was used as the threshold, and the number of grid cells with concentration values greater than the threshold was calculated and multiplied by the grid area to give the total exposure area. Similarly, the total particle concentration at each output time-step was estimated, and the mixing ratio was calculated based on the particle density. To quantify the extent of the spread of the virus blob released into the atmosphere, we determine the area (or the radius) covered by the blob and the mixing ratio, the ratio of the density of the blob with respect to the initial density of the particles.

### Characterizing the Planetary Boundary Layer

Turbulence kinetic energy (TKE) is a measure of the total energy present in an air-parcel. The turbulence developed in the PBL is due to the combined effect of the heat exchange between the atmosphere and the earth's surface (buoyancy forcings) and the interaction of the wind with the earth's surface (shear forcings). The shear production of TKE from the wind shear at the surface positively contributes to the TKE production; meanwhile, the buoyancy production from the temperature gradient or heat flux at the surface can contribute positively during unstable PBL regimes and negatively during stable regimes.

The governing length-scale in the PBL is the Monin-Obukhov length ( $L$ ) which is based on the relative contributions from shear/buoyancy production of TKE, where  $L = \frac{-u_*^2 \theta}{(\kappa g)(\overline{w'\theta'})}$ ,  $\kappa$  is the Von Karman's constant, and  $\theta$  is the mean potential temperature. It is a ratio of the shear-driven processes given by the friction velocity  $u_*$  and buoyancy-generating processes given by surface heat flux ( $\overline{w'\theta'}$ ). Here,  $\kappa$  is the Von Karman's constant, and  $\theta$  is the mean potential surface temperature.

The regimes of the PBL is classified depending on the wind speeds and the relative measure of  $L$  with respect to the PBL depth  $z$  ( $\zeta = z/L$ ), such as class A with strong convection and weak winds to class F with stable stratification and weak winds (Golder, 1972).

## 3. Results

Fifteen different instances of release conditions during the period of March 9th-April 6th under realistic meteorological conditions are analyzed (Table 1). We first investigate the transport scales of the cloud under different PBL regimes, and then analyze the role of the meteorological variables on the dynamics of transport and mixing. In Table 1 the

fifteen different instances in the analysis, are arranged from highly convective  $\zeta$  to weakly stable stratified PBL regimes. The columns correspond to  $\zeta$ , release date and time,  $T$ ,  $z$ ,  $L$ , wind-speed at 10 m height, wind shear close to the ground ( $dU/dz$ ), temperature gradient close to the ground ( $dT/dz$ ), TKE, and moisture content on the ground (amount of moisture per kg. of air).

The analysis for the release of the blob on April 2, 0700 CDT is presented here. This corresponds to a PBL regime of  $\zeta = -3.5$  (Table 1). Appendix Fig. 2 a-f shows the trajectory of the blob for times at  $t = 2$  min, 5 min, 10 min, 15 min, 20 min and 29 min after release (i.e.,  $t = 0$  min). The color maps correspond to the average concentration from 0 to 10 m above the ground overlaid on a geographical map of the region. The plan view shows the horizontal east-west and north-south directions. The (0,0) location is the blob's point of release corresponding to latitude and longitude of (74 W, 40 N), as shown by the red circle. Released as a point source at  $t = 0$ , the blob starts to move away from the point of release and also expands horizontally as it spreads. At 10 min following the release time, the direction of the blob is towards the north-west of the initial location, and at 15 min and beyond, it continues to move in that direction while growing in size. After 10 min, the blob is 2.5 km east and 1 km north of the original location, and it moves towards New Jersey at 15 min. At 29 min, it is 7 km east and 6 km north of its original location. As the blob moves, the ambient air mixes with the contaminant, diluting the blob. In this case, it takes around 30 min to be completely diluted.

The trajectory of the blob and the mixing can be explored using a micro-climate analysis at 0700 h CDT on April 2nd. WRF simulations reveal that the PBL is in a moderately convective regime characterized by a deep PBL layer of 1022 m, winds at a moderate speed of 5.2 m/s, and moderate turbulence blowing over the region. There is a cool ground temperature of 278.6 K with a moisture content of 3.5e-3 kg/kg of air, and the wind-shear is stronger than the thermal gradient on the ground (Table 1). The wind-shear and the positive temperature gradient at the surface act as sources of TKE production, resulting in the generation of TKE from both shear-driven and buoyancy-driven processes. The horizontal velocity vectors ( $u$ - $v$ ) colored with the PBL depth at release time are shown in Appendix Fig. 3a. The region is influenced by moderate winds that blow towards the ocean. Turbulence is organized as updrafts and downdrafts with a vertical velocity of around 1 m/s, as seen in Appendix Fig. 3b. The energy containing convective rolls influence the trajectory of the blob.

To understand the differences in trajectory for different release conditions, two additional sets of cases are presented with the release conditions of April 5, 0700 h CDT ( $\zeta = -5.28$ ) and March 10, 1900 h CDT ( $\zeta = 2.75$ ). WRF simulations demonstrate that the PBL exhibits different characteristics for these regimes. For example, the PBL is in a moderately convective regime; however, it is shallow in depth with low winds and weak turbulence generated from a combination of low shear-driven and low buoyancy-driven production when  $\zeta = -5.28$ . Turbulence is generated due to a small negative temperature gradient (sink of TKE production) and a positive high wind-shear (source of TKE production). Appendix Fig. 4 a-f shows the trajectory of the blob at 5 min, 10 min, 15 min, 20 min, 25 min, and 30 min after the release time. At 5 min, the blob expands in area; however, the transport of the blob is slow compared to the  $\zeta = -3.5$  case. The blob continues to move eastwards for a distance of 0.5 km and 2.5 km from the source, 10 min and 20 min after release, respectively. The region is influenced by stronger south-west marine winds and weaker circulation over the land of less than 5 m/s, resulting in an elliptical region of coverage. Appendix Fig. 5 a-f shows the trajectory of the blob released on March 10th, 1900 CDT at 2 min, 5 min, 10 min, 15 min, and 20 min after release time. The PBL is deep, representing a transition from a neutral to a stable regime. At 5 min after release, the blob moves 1 km north-east towards a densely populated area, and it continues in this direction, having moved 5 km after 20 min before mixing and becoming diluted 30 min after release. The wind patterns are extremely complicated with the convergence of

strong circulations from the marine boundary layer to the south-east, winds blowing from the north in the eastern part, and north-west winds in the western area.

In summary, the response of the blob to atmospheric turbulence is dictated by PBL characteristics, such as wind shear, temperature gradient, energy containing horizontal rolls, and turbulence. In weakly/moderately convective regimes, the PBL contains buoyancy- and shear-induced motions that influence the transport and mixing of a blob released close to the ground (2 m height). The buoyancy-induced motions form updrafts, regions of positive vertical velocity fluctuations (away from the ground direction), and downdrafts, broad regions of negative vertical velocity fluctuations (towards the ground direction). The shear-induced motions due to the wind shear form horizontal convective "rolls" – large-scale coherent structures that align with the mean wind. When released close to the ground, the virus-blob with a particle concentration  $c$  is advected by the updrafts/downdrafts vertically (towards the ground or away from the ground) that transport the cloud before it mixes with the atmosphere and becomes diluted. The flux is carried by buoyancy-induced vertical motions when released in weakly or moderately convective PBL, whereas for  $\zeta > 0$  cases, the shear-induced motions give rise to the upward flux of the virus-cloud. The shear-driven turbulence production mixes and dilutes it.

Next, we analyze the area covered by the blob as it moves in time. All fifteen cases are analyzed here. Fig. 1a shows the area covered by the virus-blob in time as it expands due to the local turbulence until it dilutes due to mixing with the atmosphere. Fig. 1b shows the mixing ratio of the blob (ratio of contaminant density at a given time to the initial density in the blob). The spreading rate at which it mixes with the ambience before dilution strongly depends on the meteorological conditions. During moderately convective conditions ( $\zeta = -5.95$ ) in a deep boundary layer with high turbulence and strong winds, the virus-cloud expands and transports quickly, e.g., covering a region of  $0.5 \times 10^5 \text{ m}^2$  (radius of 40 m) in 1 min and  $10^5 \text{ m}^2$  (radius of 180 m) in 3 min. It mixes and dilutes quickly in 25 min. However, if the boundary layer is shallow ( $\zeta = -5.28$ ) with low turbulence and gentle winds, the virus-cloud is less confined (e.g., it covers half the area of the previous state; however, it persists without diluting for a longer time). Weakly convective conditions ( $\zeta = -1.44$ - $-1.4$ - $-1.39$ ) with a shallow boundary layer and gentle winds and low turbulence results in the mixing of the virus-cloud throughout the PBL depth in the order of 200 m, causing an undiluted virus-blob to spread to a larger area for a longer amount of time. In the two cases corresponding to stable PBL regimes,  $\zeta = 0.63, 0.75$ , the PBL depth is deep and the TKE production is mainly due to the wind-shear as the contribution from buoyancy-generated TKE is very low. This suggests that these regimes represent transition from a neutral to a stable regime. The conditions are characterized by low winds of around 5 m/s and moderate shear-driven turbulence. The mixing is dictated by purely shear-driven processes. The blob expands to a maximum area of  $1.2/1.5 \times 10^5 \text{ m}^2$  (or a radius of 200/220 m) for cases  $\zeta = 2.65/0.73$ , and it persists in size for a longer time.

Next, we discuss the variations in the atmospheric stability and local climate of the New York region. The urban boundary layer in New York City is influenced greatly by the sea breeze due to the ocean's proximity. We analyze the role of local meteorological variables on the direction of transport from the initial release location and the meteorological variables that influence the direction. Fig. 2 a-d shows the diurnal variations of the PBL characteristics during the periods of March 9–14, March 20–26, and April 1–6. The period of March 9–14 is characterized by average winds of 5 m/s with an isolated event of peak winds at 10 m/s. Later, during the month of March and during the period of April 1–6, there exist significant inter-daily variations, including events of high winds of around 10 m/s and low winds of 2 m/s. The wind direction does not exhibit any specific trends, and there appear significant variations. The PBL depths are deep for a significant number of days during the day-time conditions, and they also are marked by shallow night-time conditions. The atmospheric stability parameter  $L$  shows strong diurnal

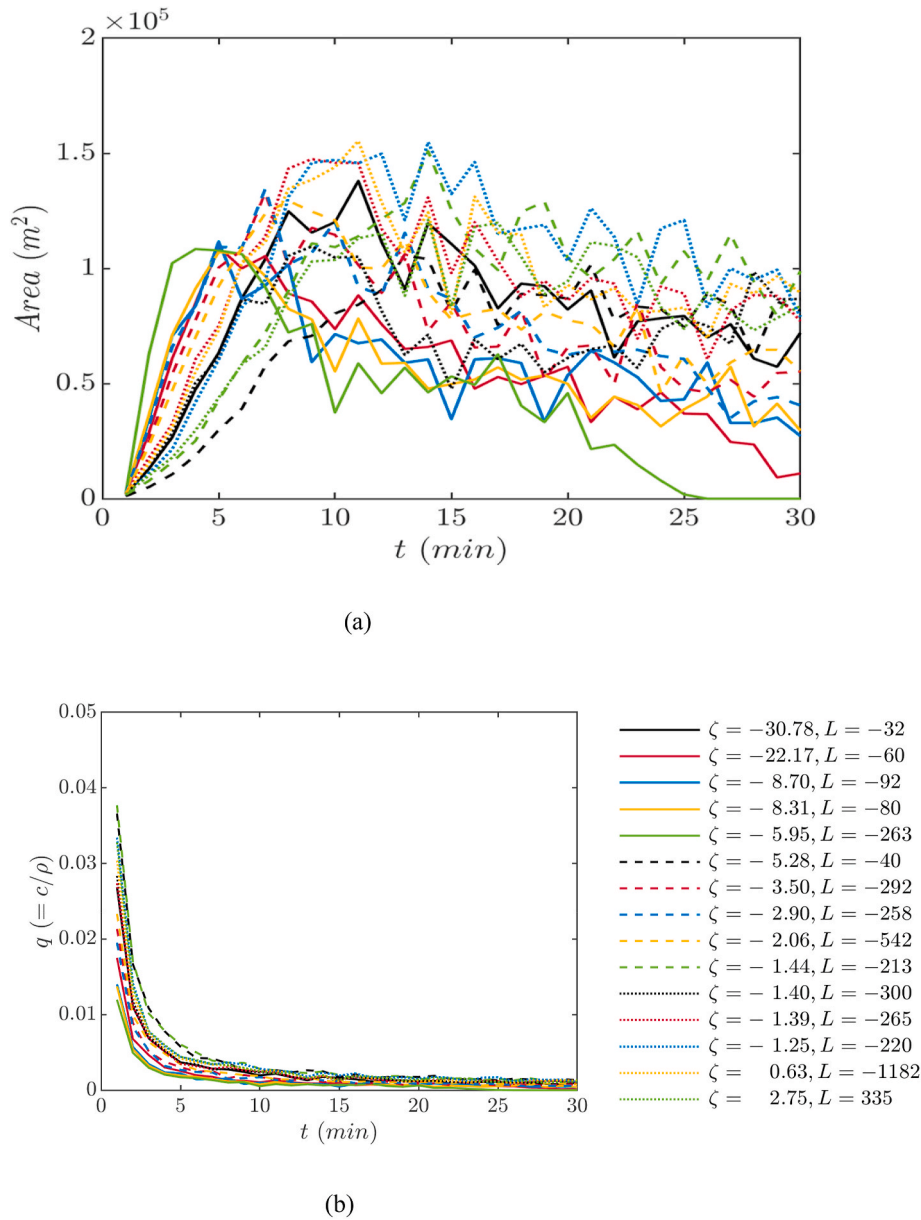


Fig. 1. (a) Region covered by the virus-cloud at times (minutes) from the time of release, (b) mixing of the pollutant with the atmosphere in time (See Table 1).

variations as the values change from positive to negative during the heating/cooling of the surface during daytime/nighttime conditions. In summary, during the analysis period, the PBL is predominantly in a convective regime, with a few instances of purely stable regimes. Turbulence in convective regimes is organized as large-scale coherent structures, which play a dominant role in transporting the blob.

Appendix Fig. 6a shows the turbulence structures in the PBL. The PBL is characterized by well-developed horizontal rolls with strong updrafts and downdrafts. The size of the rolls ( $u-w$ ) on April 4th vary; for instance, the rolls are 9 km wide and 1.5 km in height (size of each roll) at 1700, and they are 3 km wide and 1 km in height on April 3rd, 1630. The ( $v-w$ ) rolls on April 3rd are narrower but deeper with a width of 1.5 km and extending to 1.8 km deep. As seen in Appendix Fig. 6b, the ( $v-w$ ) rolls on April 3rd are narrower but deeper, with a width of 1.5 km and extending to 1.8 km deep.

4. Discussion and conclusions

A computationally intensive study has been performed to accurately

represent the dispersion processes and the factors influencing the transport and mixing of the cloud or blob of virus-filled micro-particles released due to coughing, sneezing, or similar events into the atmosphere. The motivation of the study is two-fold. First, the New York region has become the epicenter of coronavirus spread in the USA, with a steady increase in disease spread beginning in March and continuing to date. Therefore, there is an urgent need to conduct a study specific to the New York region during this period in order to gain an understanding of the key factors that correlate with the spread of the disease. Second, there is no knowledge regarding the possibility of infection spread due to coughing/sneezing and air-current conditions in the atmosphere. As such, this study provides an important direction for future research, with direct implications on social distancing protocols and face masks for protection.

Fifteen different instances of conditions corresponding to morning, afternoon and evening released during the period of March 9th-April 6th are analyzed in the New York City region. The analysis of the meteorological conditions during these time-periods has revealed the PBL to exist in three different regimes - weakly convective, moderately

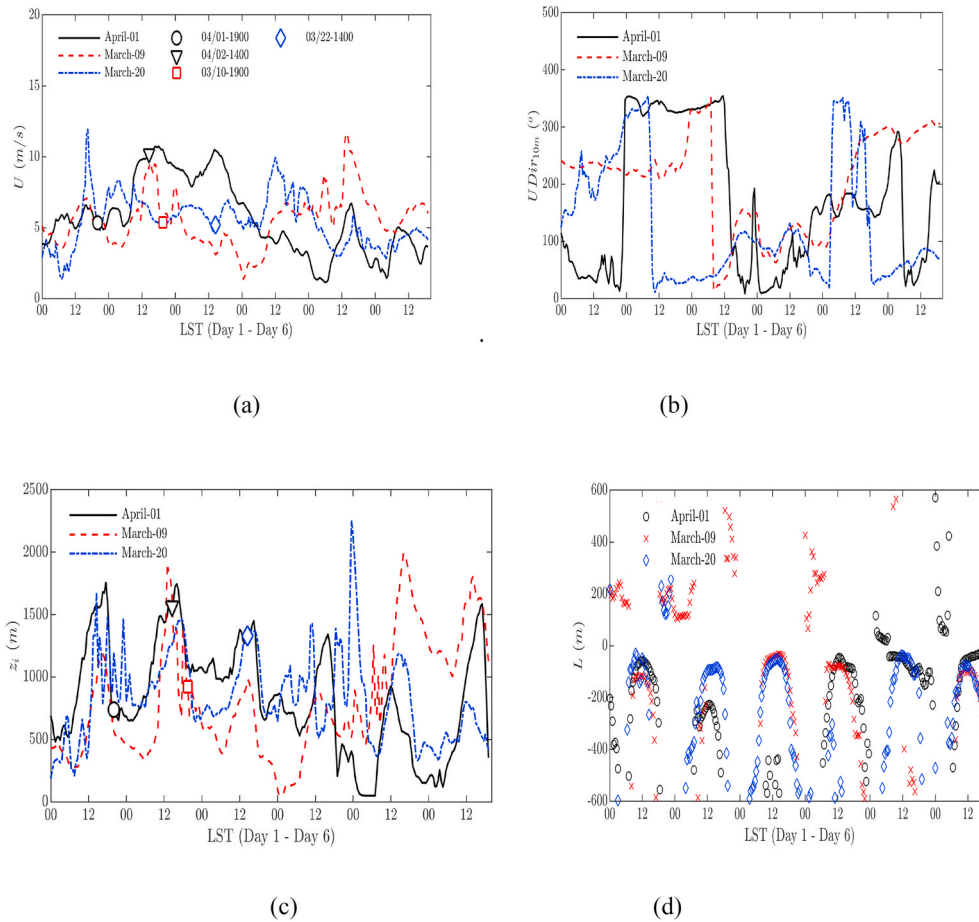


Fig. 2. WRF simulation results for periods covering March 9–16, March 22–26, April 1–6: (a) Wind speed at 10 m height, (b) Wind direction at 10 m height, (c) PBL height, (d) Scale  $L$ .

convective, and near-neutral transitioning to stable regimes - based on  $\zeta$  ( $z/L$ ). The PBL is characterized by the regime, low/high wind speeds and low/high turbulence. The strength of the PBL rolls (and hence their size), the low winds and low turbulence all together favor enhanced transport of the virus-blob as it persists in the atmosphere for a longer time. On the other hand, conditions of high turbulence rapidly mix and dilute the virus-blob quickly without transmitting the infection. Turbulence is an agent that advects (in three-dimensions) and also mixes the blob of released micro-particles. Turbulence mixing is very efficient, and the micro-particles mix with the surrounding air currents, eventually diluting the concentration of the infected particles per unit volume of air inhaled by individuals.

The findings of the study are summarized as follows:

- In weakly and moderately convective regimes, the transport direction and the extent of blob spread correlate with the wind shear and the temperature gradient, and with the scales of the horizontal rolls and thermal updrafts and downdrafts.
- In neutral conditions (or stable regimes with a deep boundary layer), the transport correlates only with the wind-shear, and the buoyancy effects do not contribute.

Overall, during the afternoon releases, the conditions such as high turbulence, strong winds and deep PBL causes the blob to be transported further away from the source location and dilutes it quickly. Such conditions are not favorable for transmission of the infection. During the morning and evening releases, the atmospheric conditions - shallow/moderately deep PBL depth, cool ground temperature (resulting in positive temperature gradient at the surface) and strong wind shear

(near the ground) with low to moderate turbulence and gentle winds - enhance the transmission of the infection due to the updraft/downdrafts of the convective rolls in the atmosphere. The wind-direction plays an important role in the direction of the transport. For instance, during the April 2, 0700 CDT release, the blob moves in a north-west direction, and it is 7 km east and 6 km north of the source at 29 min before becoming diluted. During the April 5, 0700 CDT release, the blob moves 2.5 km east in 20 min before it is diluted. Hence, the extent of the spread of the infection will depend on the population density in the path of the transport.

Recent studies have all demonstrated low average wind speed and low ambient temperature correlate with a rapid transmission of the disease in different geographical regions, including, in northern Italy (Coccaia, 2020), in Iran (Islam et al., 2020), in Southern Europe (Sanchez et al., 2020), and in tropical regions (Rosario et al., 2020). The limitations of the existing studies are that other related factors have not been included in the study. The present study adds to the existing knowledge that atmospheric stability regimes (weakly convective conditions) that result in low wind speeds, low level turbulence and cool moist ground conditions favor the transmission of the disease. Further, the wind direction is an important factor that dictates the direction of the transport. If the transport is towards a densely populated region then the air-borne transmission accelerates the spread of the disease. Due to the combination of the factors that contribute to a favorable spread of the infection, the transmission route in outdoor environments is extremely complicated to understand. Most of the exiting studies have demonstrated the dispersion as the dominant mechanism indoors for the spread of the disease (e.g. Jayaweera et al., 2020), however, depending on the combination of factors in the environment, the air-borne spread

of the disease is highly possible. The study confirms the analysis of Bontempi (2020) that it not possible to conclude that COVID-19 diffusion mechanism also occurs through the air, by using  $PM_{10}$  as a carrier. The cough/sneeze jet of an infected person is released into the atmosphere as a buoyant plume of virus-particles that mixes with the ambient turbulence and it is transported by turbulence. Hence, as shown in the study low turbulence and low winds favor the disease transmission as the virus-blob (or virus plume) survives for a few hours in the atmosphere before it being diluted and losing its potency. A recent work by Bianco et al., 2020 has demonstrated that Ultraviolet-C (UV-C) radiation has a potential for inactivation and complete inhibition of all viral concentrations. However, it should be noted that as the sunlight passed through the atmosphere all UV-C is absorbed by ozone, water vapor, oxygen and Carbon Dioxide. Hence, the natural sunlight may not have the affinity to deactivate the virus. The framework established in the current work can be extended to various geographical locations, and also explains the increasing number of cases during the hot summer months in South-West and Western United States.

The study provides robust evidence to the recent report by the National Academy of Science raising concerns about transmission of SARS-CoV-2 via aerosols generated from droplets (National Academies of Sciences, 2020). The report indicated an airflow modeling study following the SARS-CoV-1 outbreak suggesting the spread of disease as a rising plume of contaminated warm air (Yu, 2004). This study is offered as an important contribution demonstrating the role of local meteorological conditions in spreading the coronavirus, and the results demonstrate that, from the initial time of release, the virus can spread up

to 30 min in the air, covering a 200 m radius region at a time and moving to 1–2 km from the original source.

### Funding

The work has been funded by NASA MIRO Center for Advanced Measurements in Extreme Environments Grant number: 80NSSC19M0194.

### Author contributions

KB was involved in writing the manuscript, conducting the background study and detailed analysis of the results. SB was involved in performing the numerical model simulations and post-processing the data.

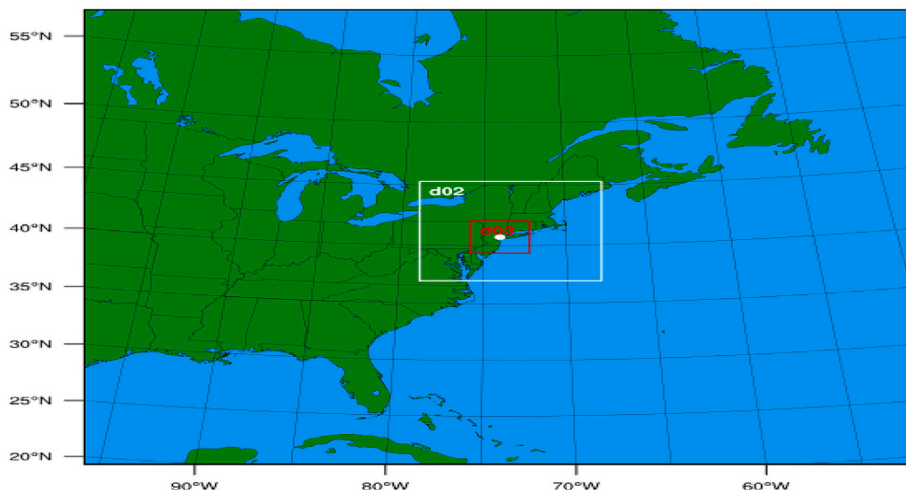
### Declaration of competing interest

The authors declare that they have no known competing financial interests or personal relationships that could have appeared to influence the work reported in this paper.

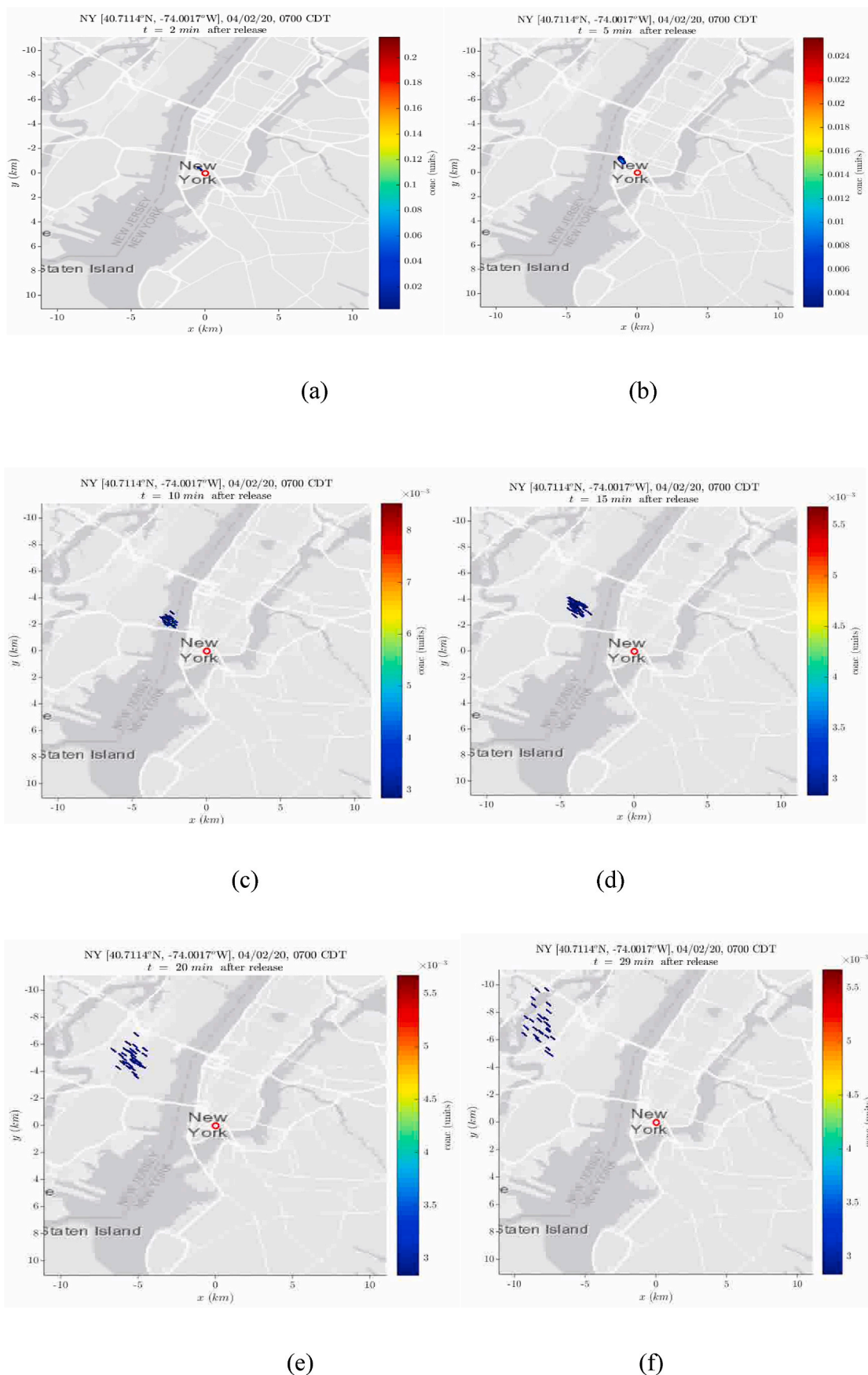
### Acknowledgments

The author acknowledge Texas Advanced Computing Center (TACC) for provide timely and valuable supercomputing facilities to conduct the simulations.

## Appendix A

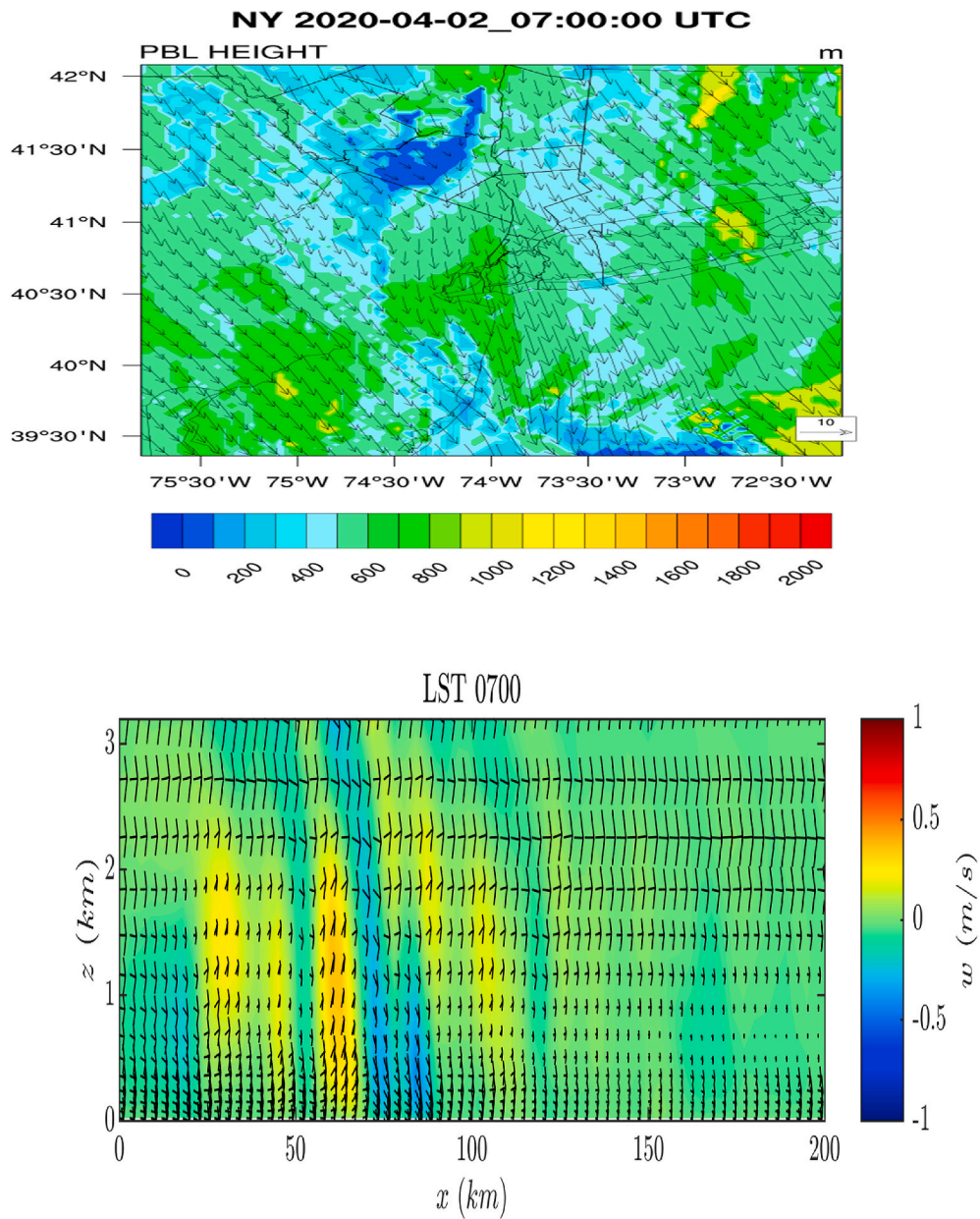


Appendix Fig. 1. Numerical domain for WRF-ARW configuration over NY (white dot). The domain consists of nested grids.

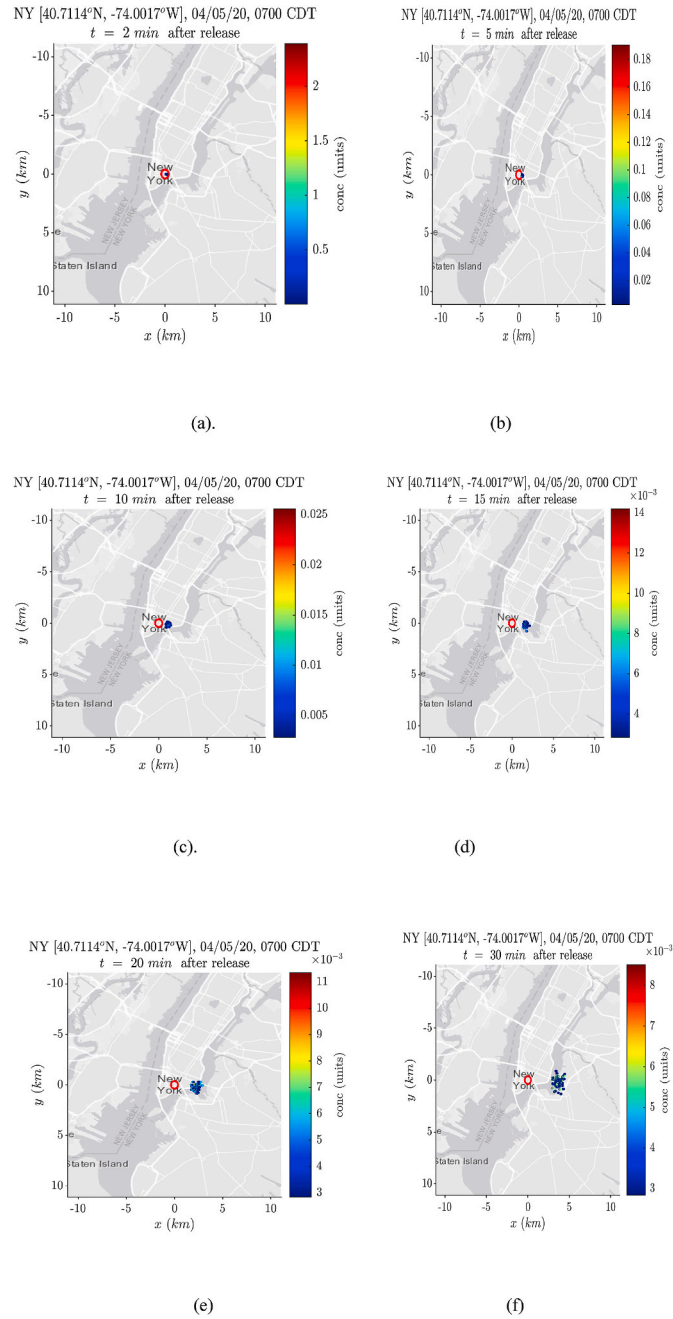


**Appendix Fig. 2.** For the April 2nd 0700 h CDT release, the trajectory of the blob released at time  $t = 0$  along the north-south and east-west plane at (a)  $t = 2$  min, (b) 5 min, (c) 10 min, (d) 15 min, (e) 20 min, (f) 29 min after the release time.





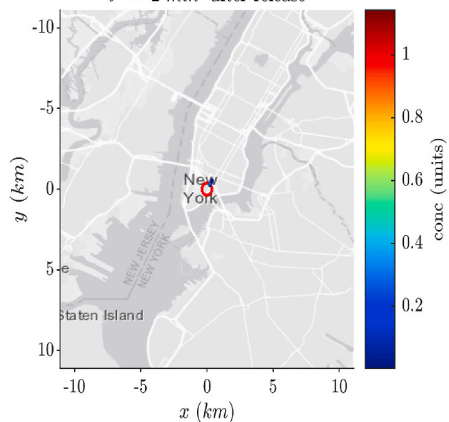
**Appendix Fig. 3.** Wind vectors for April 2, 0700 CDT hours release (a) velocity vectors in the latitude-longitude plane colored with PBL height, (b) horizontal convective rolls in  $x$ - $z$  plane.



Appendix Fig. 4. April 5, 0700 CDT Release (a) 2 min (b) 5 min (b) 10 min (c) 15 min (d) 20 min (e) 30 min

NY [40.7114°N, -74.0017°W], 03/10/20, 1900 CST

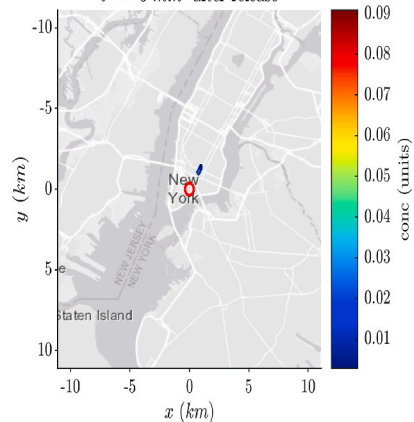
$t = 2 \text{ min}$  after release



(a)

NY [40.7114°N, -74.0017°W], 03/10/20, 1900 CST

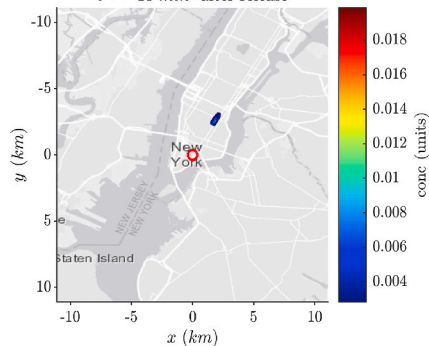
$t = 5 \text{ min}$  after release



(b)

NY [40.7114°N, -74.0017°W], 03/10/20, 1900 CST

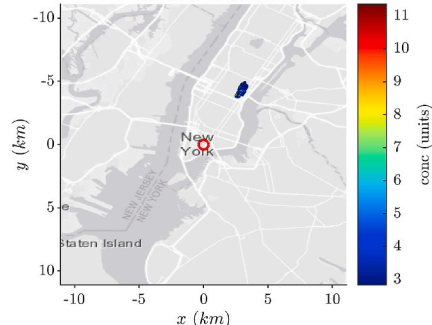
$t = 10 \text{ min}$  after release



(c)

NY [40.7114°N, -74.0017°W], 03/10/20, 1900 CST

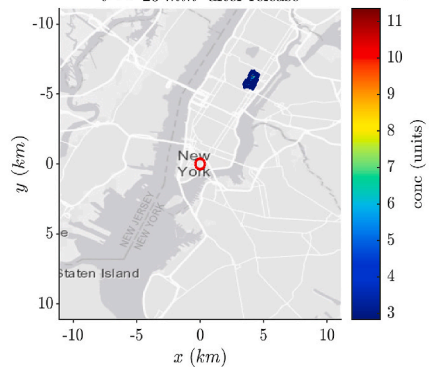
$t = 15 \text{ min}$  after release



(d)

NY [40.7114°N, -74.0017°W], 03/10/20, 1900 CST

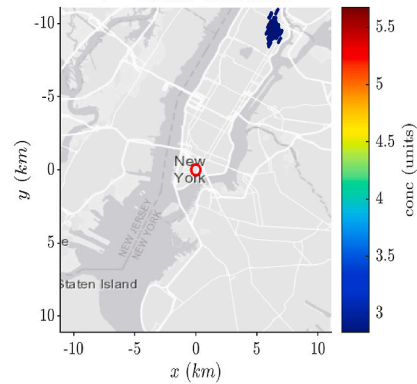
$t = 20 \text{ min}$  after release



(e)

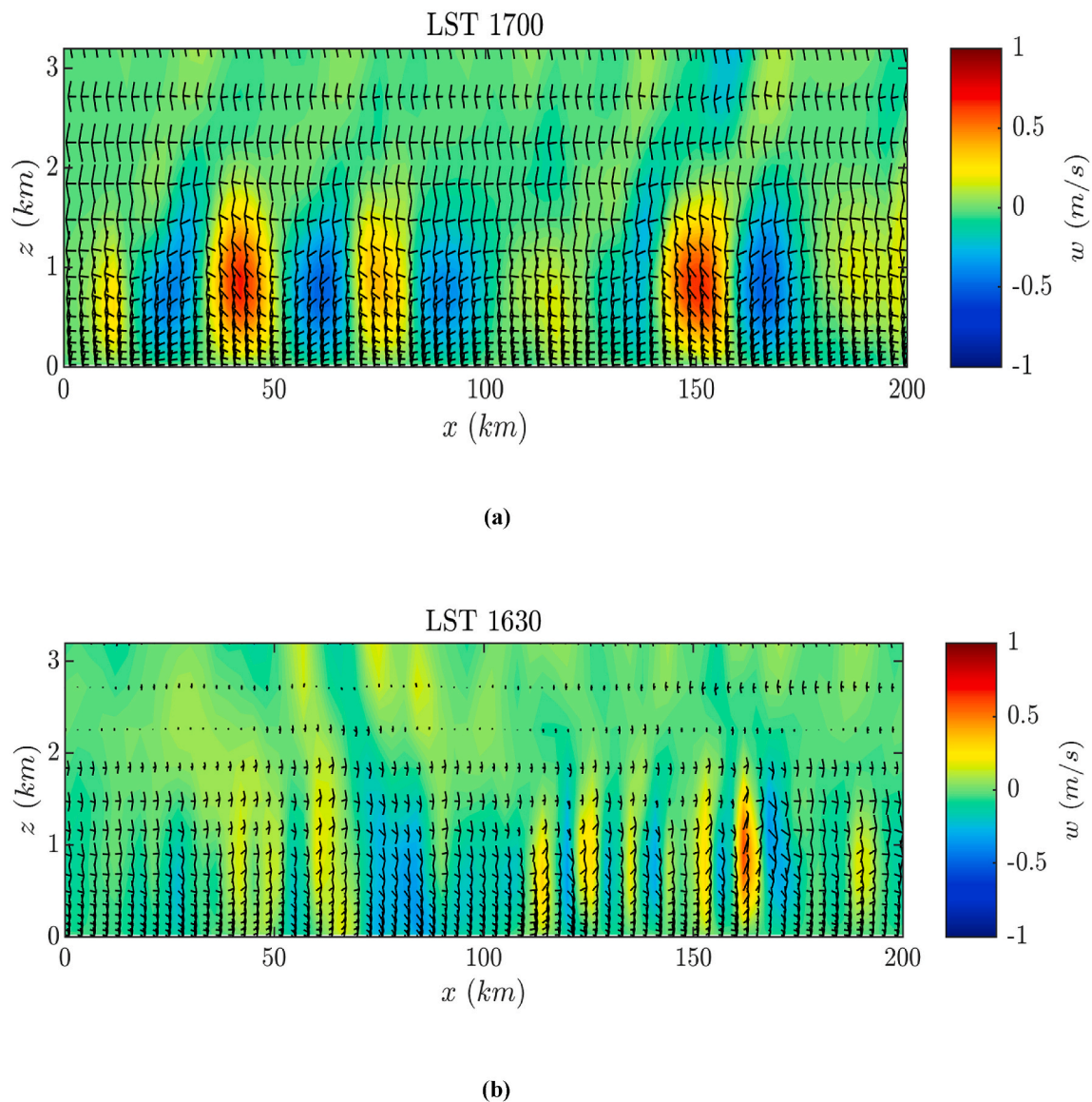
NY [40.7114°N, -74.0017°W], 03/10/20, 1900 CST

$t = 30 \text{ min}$  after release



(f)

Appendix Fig. 5. March 10, 1900 CDT Release (a) 2 min (b) 5 min (b) 10 min (c) 15 min (d) 20 min (e) 30 min.



**Appendix Fig. 6.** Horizontal roll ( $u$ - $v$  vectors colored with  $w$  contours) at different time-instants of the WRF simulations: (a) April 4, 1700 h CDT, (b) April 3, 1630 h CDT.

## Appendix B. Supplementary data

Supplementary data to this article can be found online at <https://doi.org/10.1016/j.envres.2020.110170>.

## References

- Ahmadi, M., Abbas, S., Dorost, S., Ghouschi, S., Jafarzadeh, G.N., 2020. Investigation of effective climatology parameters on COVID-19 outbreak in Iran. *Sci. Total Environ.* 729. Article 138705.
- Bhaganagar, K., Bhimoreddy, S.R., 2017. Assessment of the plume dispersion due to chemical attack on April 4, 2017, in Syria. *Nat. Hazards* 88 (3), 1893–1901.
- Bhimoreddy, S.R., Bhaganagar, K., 2018a. Short-term passive tracer plume dispersion in convective boundary layer using a high-resolution WRF-ARW model. *Atmospheric Pollution Research* 9 (5), 901–911.
- Bhimoreddy, S.R., Bhaganagar, K., 2018b. Performance assessment of dynamic downscaling of WRF to simulate convective conditions during sagebrush phase 1 tracer experiments. *Atmosphere* 9 (12), 505.
- Bianco, A., Biasin, M., Pareschi, G., Cavalleri, A., Cavatorta, C., Fenizia, F., Galli, P., Lessio, L., Lualdi, M., Redaelli, E., Saule, I., Trabattini, D., Zanutta, A., Clerici, M., 2020. UV-C Irradiation Is Highly Effective in Inactivating and Inhibiting SARS-CoV-2 Replication (June 5, 2020).
- Bontempi, E., 2020. First data analysis about possible COVID-19 virus airborne diffusion due to air particulate matter (PM): the case of Lombardy (Italy). *Environ. Res.* 186, 109639.
- Bourouiba, L., Dehandschoewercker, E., Bush, J.W.M., 2014. Violent respiratory events: on coughing and sneezing. *J. Fluid Mech.* 745, 537–563.
- Brown, R.A., 1980. Longitudinal instabilities and secondary flows in the planetary boundary layer: a review. *Rev. Geophys.* 18 (3), 683–697.
- Carleton, T., Meng, K.C., 2020. Causal Empirical Estimates Suggest COVID-19 Transmission Rates Are Highly Seasonal medRxiv.
- Coccia, M., 2020a. Factors determining the diffusion of COVID-19 and suggested strategy to prevent future accelerated viral infectivity similar to COVID. *Sci. Total Environ.* 729. Article Number: 138474.
- Coccia, M., 2020b. Two mechanisms for accelerated diffusion of COVID-19 outbreaks in regions with high intensity of population and polluting industrialization: the air pollution-to-human and human-to-human transmission dynamics. medRxiv 2020, 2020.04.06.20055657.
- Coccia, M., 2020c. The effects of atmospheric stability with low wind speed and of air pollution on the accelerated transmission dynamics of COVID-19. *Journal: International Journal of Environmental Studies GENV*. Article ID: GENV 1802937.

- Centers for Disease Control and Prevention, 2020. Coronavirus Disease 2019 (COVID-19): Symptoms of Coronavirus. <https://www.cdc.gov/coronavirus/2019-ncov/symptoms-testing/symptoms.html>. (Accessed 22 June 2020).
- Coronavirus disease (COVID-2019), 2020. Situation reports (Accessed 8th of April 2020. <https://www.who.int/emergencies/diseases/novel-coronavirus-2019/situation-reports>).
- Eslami, H., Jalili, Mahrokh, 2020. The role of environmental factors to transmission of SARS-CoV-2 (COVID-19). *Amb. Express* 10 (92), 1–8.
- Ficetola, G.F., Rubolini, D., 2020. Climate affects global patterns of COVID-19 early outbreak dynamics. *medRxiv* 2020, 2020.03.23.20040501 2020.
- Golder, D., 1972. Relations among stability parameters in the surface layer. *Boundary-Layer Meteorol.* 3, 47–58.
- Islam, N., Shabnam, S., Erzurumluoglu, A.M., 2020. Temperature, humidity, and wind speed are associated with lower Covid-19 incidence. *medRxiv* 2020, 2020.03.27.20045658.
- Jayaweera, M., Perera, H., Gunawardana, B., Manatunge, J., 2020. Transmission of COVID-19 virus by droplets and aerosols: a critical review on the unresolved dichotomy. *Environ. Res.* 188, 109819.
- Lindsley, W.G., Pearce, T.A., Hudnall, J.B., Davis, K.A., Davis, S.M., Fisher, M.A., et al., 2012. Quantity and size distribution of cough-generated aerosol particles produced by influenza patients during and after illness. *J. Occup. Environ. Hyg.* 9, 443–449.
- Moeng, C.-H., Sullivan, P., 1994. A comparison of shear- and buoyancy-driven planetary boundary-layer flows. *J. Atmos. Sci.* 51, 999–1022.
- National Academies of Sciences, April 1 2020. Engineering, and Medicine 2020. Rapid Expert Consultation on the Possibility of Bio Aerosol Spread of SARS-CoV-2 for the COVID-19 Pandemic. The National Academies Press, Washington, DC.
- Rosario, D.K.A., Mutz, Y.S., Bernardes, P.C., Conte-Junior, C.A., 2020. Relationship between COVID-19 and weather: case study in a tropical country. *Int. J. Hyg Environ. Health* 229, 113587.
- Sanchez-Lorenzo, A., Vaquero-Martinez, J., Calbo, J., Wild, M., Santurtun, A., Lopez-Bustins, J.-A., 2020. Anomalous Atmospheric Circulation Favored the Spread of COVID-19 in Europe, *medRxiv*.
- Sarmadi, M., Marufi, N., Kazemi Moghaddam, V., 2020. Association of COVID-19 global distribution and environmental and demographic factors: an updated three-month study. *Environ. Res.* 188, 109748.
- Stull, R.B., 1993. Review of non-local mixing in turbulent atmospheres: transient turbulence theory. *Boundary-Layer Meteorol.* 62, 21–96.
- Van, D., Neeltje Bushmaker, T., Morris, D.H., et al., 2020. Aerosol and surface stability of SARS-CoV-2 as compared with SARS-CoV-1. *N. Engl. J. Med.* 382, 1564–1567.
- Yu, et al., 2004. Evidence of airborne transmission of the severe acute respiratory syndrome virus. *N. Engl. J. Med.* 350, 1731–1739.